Electronic Supplementary Information

Hybrid Nanostructure of SiO_2@Si with Au-Nanoparticles for Surface Enhanced Raman Spectroscopy

Huan Yang, [†] *Ben Q. Li,* [*,§,†] *Xinbing Jiang,*[†] *and Jinyou Shao*[†]

[†]Micro- and Nano-manufacturing Research Center, State Key Laboratory for Manufacturing Systems Engineering, Xi'an Jiaotong University, 28 Xianning Road, Xi'an 710049, China.

[§]Department of Mechanical Engineering, University of Michigan-Dearborn, Dearborn, MI 48128 USA.

benqli@umich.edu (Ben Q. Li)

1. SEM of Au decorated SiO_2@Si core shell particles array

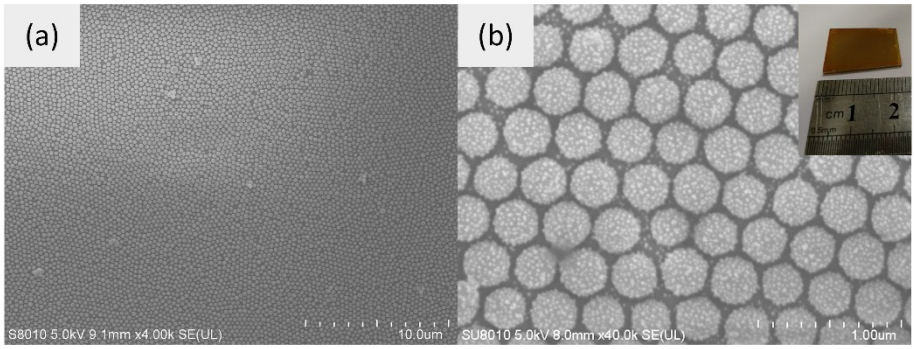

Figure S1. SEM of Au nanoparticles (d = 20nm) decorated SiO_2@Si nanoparticles with outer diameter of D = 290 nm; inset is the digital image of the sample.

2. The structural details of the SiO_2@Si core shell particle.

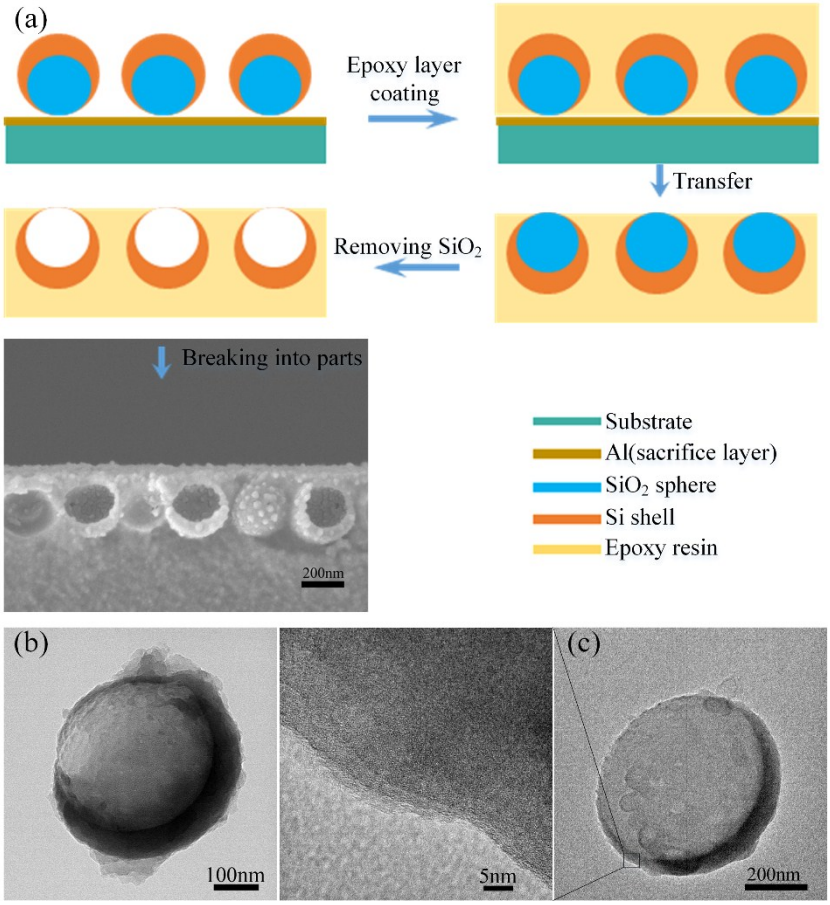

Figure S2. Images of SiO2@Si core shell particles, a) the schematic of obtaining cross section of Si shell array and SEM image of D=220/290nm SiO2@Si core shell particles array, the TEM images of (b) D=360/430nm and (c) D=560/630nm SiO_2@Si core shell particles,

The structure details of the SiO_2@Si core shell particles were examined by the SEM investigation of the particles' cross section. It was difficult to directly cut off the

particles of the samples to obtain the cross section information because the particles was settled on the substrate independently. Therefore, As Figure S3 shows, the particles array were transferred onto a polymer film to obtain the Si shell cross section by removing the SiO_2 core and break the polymer film in parts. The SEM image of the Si shell structure was shown in the Figure S2, in which the thickness increases to ~ 60 nm from the North Pole to the South of the shell.

The other two core shell particles (D=360/430nm and D=560/630nm) were characterized by TEM. The Si shell particles colloid was prepared by firstly immersing the particle array substrate in 5 % (v/v) HF to remove the SiO2 particles and separate the Si shell particle from the substrate. Then the Si shell was re-dispersed in ethanol and finally examined by HRTEM. Figure 2b and c shows the TEM images of the D=360/430nm and D=560/630nm Si shell particles, which are in the shape of crescent shell. The size of Si shell can be clearly identified in these images. Therefore, the Si shell sizes agree well with the diameters mentioned in the manuscript. The inner cavity of the Si shell seems like non-spheroid, especially for the D=560/630nm Si shell, because of the non-uniform etching of SiO_2 particles array. There was no distinct ordered crystal lattices found in the detailed examination of Figure 2b. Therefore, the PECVD deposited Si shell is amorphous silicon in this work.

3. Au particles characterization.

The size and monodispersity of the Au particles were examined by dynamic light scattering (DelsaNano C). The absorption spectra were measured by a Shimadzu UV3600 UV−Visible / NIR spectrophotometer. Since the prepared particles was

stabilized with electric double layer, the measured diameter by dynamic light scattering was a little larger than the actual size determined by SEM.

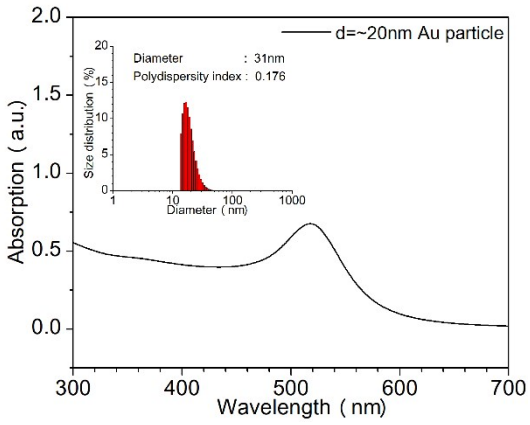

Figure S3. The absorption spectra and size distributions of prepared Au colloid used in the structure of the metal Au particles decorated SiO_2@Si core shell array.

4. Simulation model of Au decorated SiO_2@Si core shell particles

As Figure S4 shows, the structure was approximately designed by the Boolean subtraction of a silicon sphere of D = 290 nm by a SiO_2 sphere of 220nm with off-center distance e = 25 nm to exactly visualize the structure of fabricated SiO_2@Si shell as Figure S2 shows.[1] Therefore, the maximum shell thickness of the shell was 60nm in the upper of the core shell particles. Periodic boundary conditions were then applied in the x and y directions, and equator of the Si shell along XZ and YZ planes were placed with Au particles in 20 nm diameter to simplify the model.

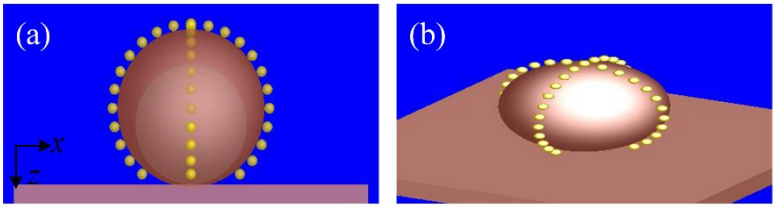

Figure S4. Side (a) and perspective (b) views of Au particles decorated SiO_2@Si core shell particle.

5. The simulated scattering curves of SiO_2@Si spherical and ellipsoid shell.

The scattering of D=220/290nm SiO_2/Si ellipsoid core shell particles with a dimeter of D_z=210/280nm in z direction was simulated and compared with the spherical one. As Figure S5 shows, the scattering peak of the ellipsoid particles was blue-shifted compared with spherical particles. It is suggested the non-spherical core shell particles indeed caused the blue shift of the scattering curve. Therefore, it can be concluded the blue shift of the calculated scattering and measured reflectance of the particles is due to the non-spherical particles.

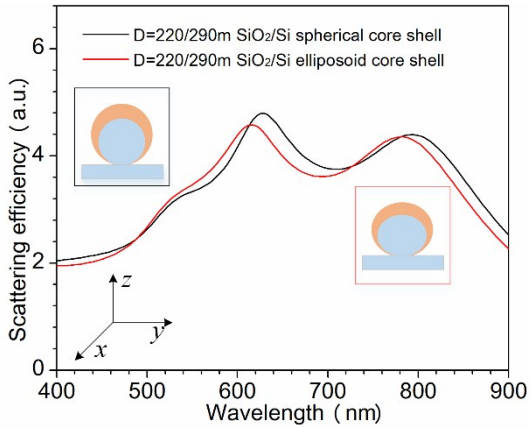

Figure S5. The simulated scattering curves of D=220/290nm SiO_2@Si spherical and ellipsoid shell.

6. Electric field distribution of SiO_2@Si core shell particles with or without Au particles

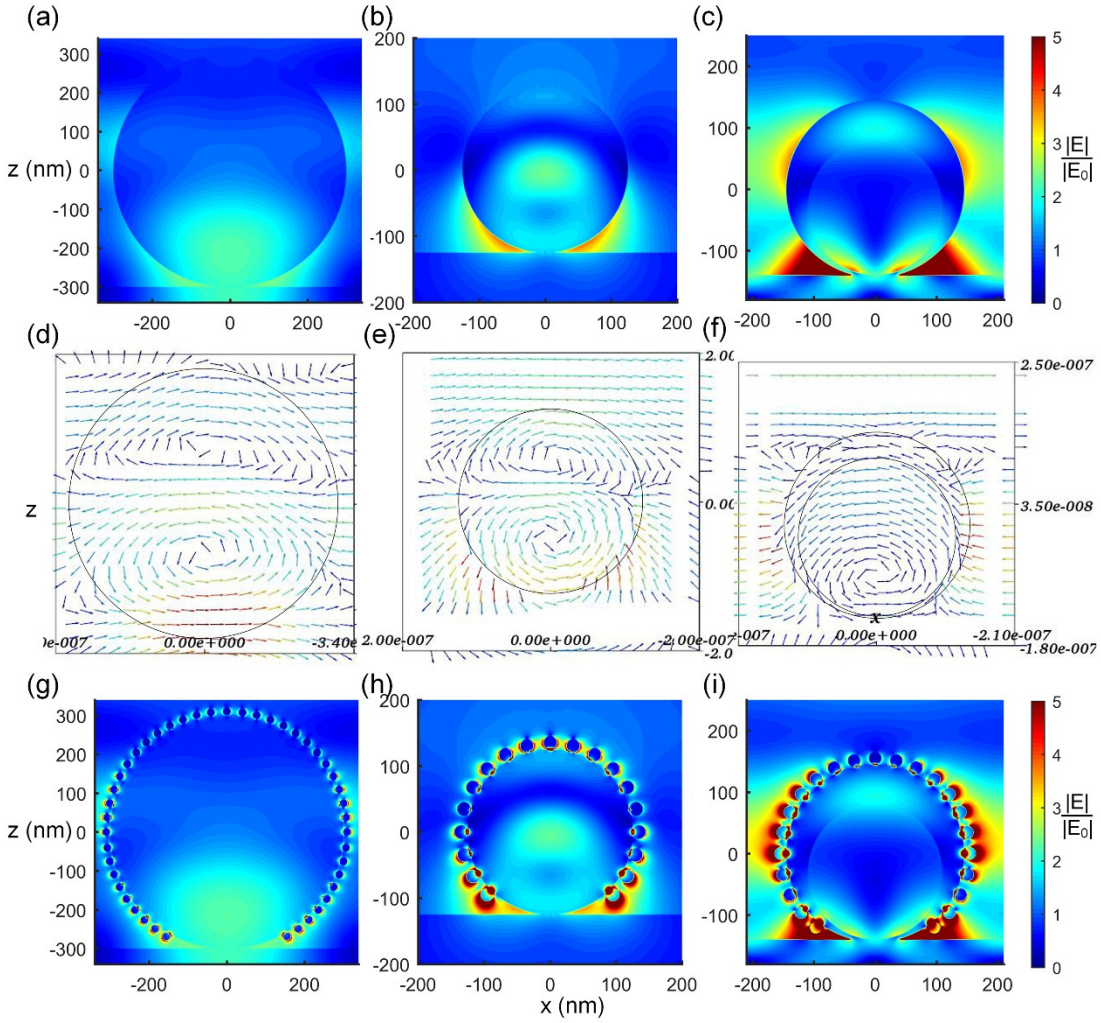

Figure S6. Electric field of particles excited by 633nm laser (a, d, g for SiO_2 sphere, b, e, h for Si sphere and c, f, i for SiO_2@Si core shell particle). The calculated electric field distribution of the E-k (x-z) plane (a-c) and magnetic quadrupole induced displacement current (d-f) inside the *D*=600nm SiO_2, *D*=250nm Si sphere and *D*=220/290nm SiO_2@Si core shell particles. (g-i) The electric field distribution of Au decorated *D*=600nm SiO_2, *D*=250nm Si sphere and *D*=220/290nm SiO_2@Si core shell particles.

7. SEM of 20nm Au decorated D=600nm SiO_2 particles array

The Au decorated SiO_2 array was prepared by electrostatic attraction discussed in the paper, because SiO_2 particles can also be modified with hydroxyl (-OH) with piranha solution. Figure S7 shows the prepared Au decorated D=600nm SiO2 particles array.

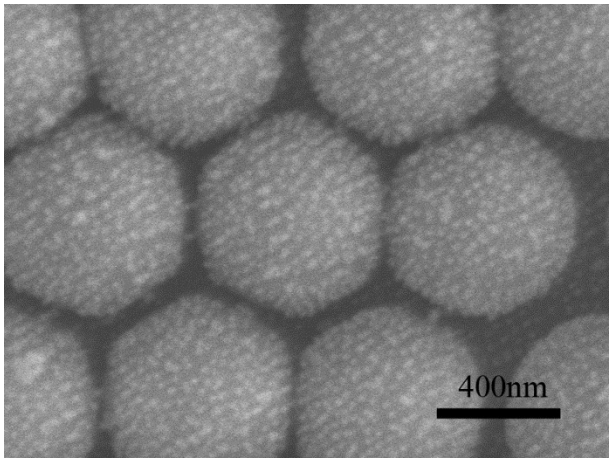

Figure S7. SEM image of 20nm Au decorated D=600nm SiO2 array.

8. D=290nm SiO2 and Si sphere examination.

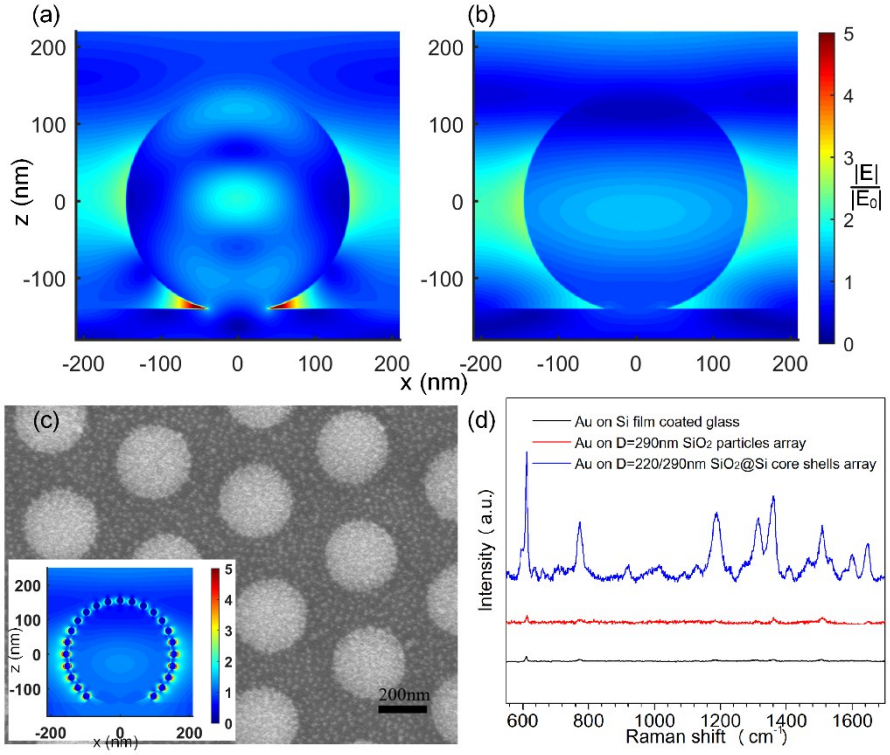

Figure S8. The simulated electric field distribution of a D = 290nm Si sphere (a) and SiO_2 sphere (b) at λ=633nm, and the SEM image (c) of Raman spectra (d) of D=290nm SiO_2 particles. Inset of Figure S8c is the simulated electric field of Au decorated D=290nm SiO_2 particle at λ=633nm.

The electric field distributions of D=290nm SiO_2 and Si sphere were simulated by FDTD solution. As Figure S8a and b shows, the local electric field of the SiO_2 or Si sphere is not impressive compared with D=220/290nm SiO_2@Si shell particles. The

sample of Au decorated on D=290nm SiO_2 particle was also prepared and examined by Raman measurement (see Figure S8c and d). It was found that the electric field of Au decorated D=290nm SiO_2 is not enormouly enhanced (see inset of Figure S8c). The measured Raman signal show no enhancement and the the intensity is just comparable to the case of Au on flat Si film, which agree well with the simulated electric field.

9. Raman detection of crystal violet by the Au decorated SiO_2@Si core shell array

In order to examine the universality of the Au decorated SiO_2@Si core shell array in Raman sensing, the crystal violet was used as the second target molecule. The samples were soaked in crystal violet aqueous solution with a concentration of 10^{-5} M for 3 hours and then thoroughly rinsed by ultrapure water. And the detection parameters were in consistent with the case of R6G introduced in the manuscript. As Figure S7a shows, When detecting by 633nm laser, the sample of *D*=220/290nm SiO_2@Si core shell array achieves the more enhanced Raman intensity than the other cases. And for 785nm laser, the sample of *D*=360/430nm SiO_2@Si core shell array perform best (see Figure S7b). The measured Raman curves agree well with the FDTD-calculated scattering and electric field intensities discussed in the manuscript. Therefore, it may be concluded that the samples of Au decorated SiO_2@Si core shell array are commonly practical for us in Raman sensing.

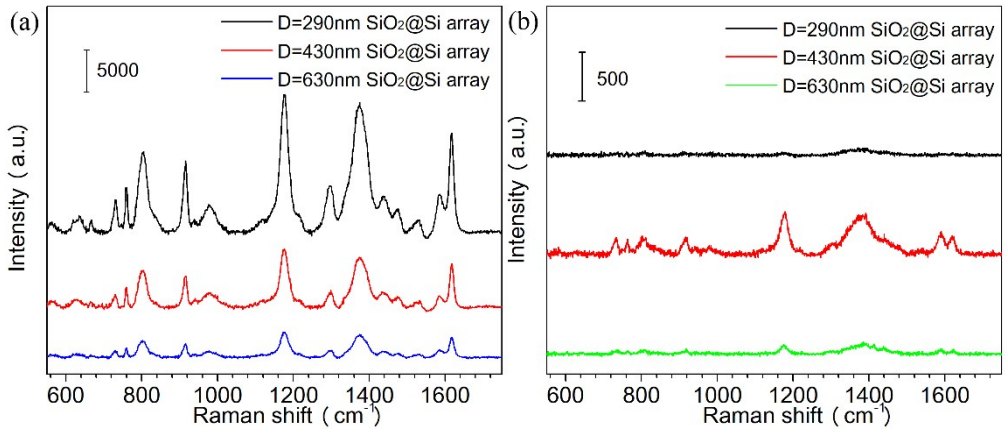

Figure S9. Raman spectra of crystal violet on Au particle decorated SiO_2@Si arrays excited by (a) 633nm laser with power of 0.35mW and (b) by 785nm laser with power of 1.5mW.

10. Enhancement factor (EF) calculation

The EF of R6G on Au decorated SiO_2@Si shell array was calculated using the following formula $EF = \left(\frac{I_{SERS}}{I_{RS}} \times \frac{N_{RS}}{N_{SERS}} \times \frac{P_{RS}}{P_{SERS}} \times \frac{t_{RS}}{t_{SERS}} \right)$ at Raman peak of 613 cm^{-1}.[2, 3]

The subscript *SERS* and *RS* represent the cases of Raman signal of R6G on the designed structure and normal Raman of R6G, respectively. In our case, the normal Raman intensity was obtained from detecting the R6G solid film on clean silicon wafer. I_{SERS} is the enhanced Raman intensity of measured molecules, while I_{RS} represents the common Raman intensity of molecules without enhancement. N_{SERS} is the number of molecules involved in the measurement of enhanced Raman intensity, while the N_{RS} represents the number of molecules in the normal Raman intensity detecting with enhancement structure. *P* and *t* represent the laser power and integration time in a single Raman measurement.

The N_{RS} denoting the average number of molecules in the scattering volume by the normal Raman experiment. We used the R6G solid powder film to finish the normal

Raman measurement, which is widely applied to estimate and calculate N_{RS}. the molecule number N_{RS} can be obtained by the commonly used equation $N_{RS} = m_{R6G} \cdot N_A / M$, where m_{R6G} is the mass of R6G powder film illuminated in the Raman measurement, N_A represents Avogadro's number and M is the molar mass of R6G.[3-11]

It was then calculated by the equation

$$N_{RS} = m_{R6G} \cdot N_A / M = V_{R6G} \cdot \rho_{R6G} \cdot N_A / M = S_{spot} \cdot T \cdot \rho_{R6G} \cdot N_A / M ,$$

where S_{spot} is the area of the laser illuminated on the sample, T is the penetration depth of the R6G solid film by the laser, ρ_{R6G} is the density of the R6G powder. The S_{spot} can be determined by $S_{spot} = \pi \left(0.61\lambda / N.A.\right)^2$, where N.A. is the numerical aperture of the objective of the Raman microscopy.

N_{SERS} denotes the adsorbed molecules in the scattering volume for the SERS experiments. It was found that the sample was coated by a monolayer of R6G molecule and the area of single R6G was 2.22nm^2, when the samples was immersed in 10^{-4} M R6G solution for 3h as prepared in our manuscript.[10-16] We followed Pan et al and Yue et al's method to obtain N_{SERS} by the equation $N_{SERS} = S_{Au} / S_{R6G}$, where the S_{Au} is the illuminated area of all Au particles and S_{R6G} is area of a R6G molecule.[10, 11]

By applying the parameters P_{RS}=0.07mW, P_{SERS}=0.35mW, t_{RS}=15s, t_{SERS}=5s, I_{RS}=57, I_{SERS}=3212, λ=633nm, ρ_{R6G}=1.17g/cm^3, M_{R6G}=479.01g/mol, $N.A.$=0.9, T=4μm, D_{Au}=20nm, Interparticle distance of neighboring Au particles is ~30nm, the final calculation of EF_{Au} (613 cm^{-1}) = ~2.2×10^8.

References

1. H. Yang, B. Q. Li, X. Jiang, W. Yu and H. Liu, *Nanotechnology*, 2017, 28, 505301.

2. E. C. Le Ru, E. Blackie, M. Meyer and P. G. Etchegoin, *The Journal of Physical Chemistry C*, 2007, 111, 13794-13803.

3. M. Chirumamilla, A. Toma, A. Gopalakrishnan, G. Das, R. P. Zaccaria, R. Krahne, E. Rondanina, M. Leoncini, C. Liberale, F. De Angelis and E. Di Fabrizio, *Advanced Materials*, 2014, 26, 2353-2358.

4. D. Lin, Z. Wu, S. Li, W. Zhao, C. Ma, J. Wang, Z. Jiang, Z. Zhong, Y. Zheng and X. Yang, *ACS Nano*, 2017, 11, 1478-1487.

5. W. B. Cai, B. Ren, X. Q. Li, C. X. She, F. M. Liu, X. W. Cai and Z. Q. Tian, *Surface Science*, 1998, 406, 9-22.

6. W.-L. Zhai, D.-W. Li, L.-L. Qu, J. S. Fossey and Y.-T. Long, *Nanoscale*, 2012, 4, 137-142.

7. Y. Peng, L. Qiu, C. Pan, C. Wang, S. Shang and F. Yan, *Electrochimica Acta*, 2012, 75, 399-405.

8. X. Wang, X. Zhu, H. Shi, Y. Chen, Z. Chen, Y. Zeng, Z. Tang and H. Duan, *ACS applied materials & interfaces*, 2018, 10, 35607-35614.

9. J. A. Huang, Y. Q. Zhao, X. J. Zhang, L. F. He, T. L. Wong, Y. S. Chui, W. J. Zhang and S. T. Lee, *Nano Lett*, 2013, 13, 5039-5045.

10. R. Pan, Y. Yang, Y. Wang, S. Li, Z. Liu, Y. Su, B. Quan, Y. Li, C. Gu and J. Li, *Nanoscale*, 2018, 10, 3171-3180.

11. W. Yue, Z. Wang, J. Whittaker, F. Lopez-royo, Y. Yang and A. V. Zayats, *Journal of Materials Chemistry C*, 2017, 5, 4075-4084.

12. A. Kudelski, *Chemical Physics Letters*, 2005, 414, 271-275.

13. J. Chen, B. Shen, G. Qin, X. Hu, L. Qian, Z. Wang, S. Li, Y. Ren and L. Zuo, *The Journal of Physical Chemistry C*, 2012, 116, 3320-3328.

14. Y. Lee, H. Kim, J. Lee, S. H. Yu, E. Hwang, C. Lee, J.-H. Ahn and J. H. Cho, *Chemistry of Materials*, 2016, 28, 180-187.

15. M. Baia, L. Baia, S. Astilean and J. Popp, *Applied Physics Letters*, 2006, 88, 143121.

16. Y.-W. Chen, T.-Y. Liu, P.-J. Chen, P.-H. Chang and S.-Y. Chen, *Small*, 2016, 12, 1458-1468.